Fluorescence anisotropy excitation by polarization shaped laser pulses after a kagome fiber

J. Otto, A. Patas, J. Althoff, and A. Lindinger

Institut für Experimentalphysik, Freie Universität Berlin, Arnimallee 14, D-14195 Berlin, Germany

Received: date / Revised version: date

Abstract We report improved fluorescence contrast between dyes by two-photon excitation with polarization shaped laser pulses after a kagome fiber utilizing the anisotropy of the dye molecules. Particularly phase and polarization tailored pulse shapes are employed for two-photon excited fluorescence of dyes in a liquid environment at the distal end of the kagome fiber. The distortions due to the optical fiber properties are precompensated in order to receive predefined polarization shaped laser pulses after the kagome fiber. This enables to optimally excite one dye in one polarization direction and simultaneously the other dye in the other polarization direction. The presented method has a high potential for endoscopic applications due to the unique properties of kagome fibers for guiding ultrashort laser pulses.

1 Introduction

Laser pulse shaping for control of photo-induced molecular processes has attained considerable success in recent years. It became most exciting when pulse shaper set-ups were employed to generate tailored laser pulses, which drive the induced processes at a maximum yield along desired paths [1,2]. In recent years polarization pulse shaping was explored in order to examine the vectorial character of the light field [3,4]. Novel pulse shaping schemes for simultaneous phase, amplitude, and polarization control were designed, and a parametric subpulse encoding was developed [5]. In this approach, the physically intuitive parameters like chirps and polarization states of subpulses can be controlled. This yields new perspectives of utilizing all properties of the light field in the pulse modulation. Recently, pulse shaping methods were increasingly used in life sciences in order to investigate biologically relevant systems. Thereto, laser pulse shaping is particularly applied

to multi-photon excitation where intrapulse interference is relevant, which enables to exploit interference effects in multi-photon excited fluorescence spectroscopy [6]. This allows for three-dimensional imaging by multi-photon microscopy e.g. for conducting cancer diagnosis [7].

In order to operate in realistic environments, methods are demanded were the light is guided to the place of interest. This is realized by transmission of light through optical fibers for endoscopic applications like medical endoscopic imaging and treatment. Yet, it is challenging to transfer laser pulses through fibers due to distortion by the optical fiber properties. This is overcome by precompensation using a pulse shaper to transmit tailored pulses through optical fibers. Moreover, parametrically shaped pulses were achieved after the fiber [8]. This enables to steer molecular processes by utilizing these pulses for inducing specific multi-photon processes in molecular systems.

This contribution reports on pulse shaping methods to control multiphoton processes after transmitting a microstructured kagome fiber. Kagome fibers are favorable for guiding ultrashort laser pulses, because they sustain high intensities and transmit a broad frequency band [9–11]. Precompensation of pulse distortions due to fiber transmission is conducted with the pulse shaper in order to receive specific parametric pulse forms after the fiber. The tailored laser pulses cause selective multiphoton induced fluorescence of dye mixtures. Special antisymmetric phase functions will be employed for scans of the multiphoton excitation fluorescence [12]. The application of phase and polarization tailored pulses for imaging contrast enhancement is demonstrated for dye molecules in a liquid after transmitting a nanostructured kagome fiber. Laser pulse shaping of multiphoton excitations after novel optical fibers has a high potential for new biophotonic applications in endoscopy and microscopy.

2 Experimental setup

A schematic of the experimental setup is depicted in fig. 1. The laser pulses are generated by a femtosecond oscillator (Mira, Coherent) producing pulses with an energy of 6 nJ at a repetition rate of 76 MHz. The spectrum measures 32 nm in width (FWHM) at a central wavelength of 805 nm and is close to Gaussian in shape. The pulse shaper consists of a zero dispersion compressor in a symmetric 4-f configuration. The pulses are dispersed by gratings with 1200 lines/mm and are focused in the Fourier plane by cylindrical lenses of 250 mm focal length. In the Fourier plane, the spectrally separated frequency components are modulated by a double liquid crystal array modulator (SLM-640, Cambridge Research Instruments) with two liquid crystal arrays with their optical axes oriented at $\pm 45°$. This setup is capable of simultaneously and independently modulating phase and polarization of the laser pulses, or of phase and amplitude by adding a polarizer behind the modulator. The two arrays of the shaper can be used to generate

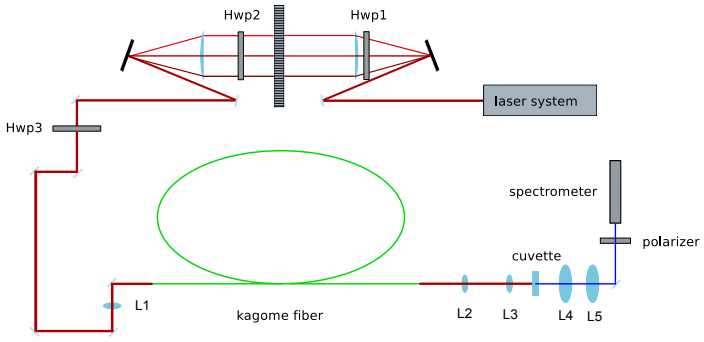

Fig. 1 Experimental setup. The installed lenses are denoted by L1 to L5 and the half wave plates by Hwp1 to Hwp3.

two perpendicular linear polarized independently shaped pulses parallel to the axes of the arrays. Thereto, the phase functions are written separately on each array which provides phase shaped pulses for both polarization directions because the optical axes of the two arrays are perpendicular to each other. Hence, the phase function of one array provides the pulse shape in one polarization direction and the phase function on the other array generates the other pulse shape in the other polarization direction. These polarization components can moreover be delayed with respect to each other. Two half-wave plates (Hwp1, Hwp2) are added to the setup. The one (Hwp1) before the cylindrical lens of the pulse shaper is issued to compensate for different reflectivities in horizontal and vertical polarization. The other half wave plate (Hwp2) is placed directly after the SLM-640 to rotate the polarization of the pulses from +45° and 45° to 0° and 90°. For the measurements with only a linearly polarized pulse, a polarizer is placed behind the setup to select one polarization component.

The light is focused with a f = 150 mm lens (L1) into the kagome fiber (PMC-PL-780-USP from GLOphotonics SAS). The image and the transmission of the 4 ring 7 cell hypocycloid core kagome fiber are shown in fig. 2. The fiber has a core diameter of 55/70 μm, an outer diameter of 400 μm, and a numerical aperture of 0.009 [13]. The coupling into the fiber can be adjusted with the two previous mirrors and also the angle of one end of the fiber can be varied. After transmitting the fiber the light is parallelized by another lens (L2) with a focal length of 300 mm. In order to have high intensities the shaped pulses are focused with a f = 100 mm lens (L3) into a cuvette filled with the dyes rhodamine B ($rhoB$) and coumarin 1 ($cou1$) (also named coumarin 47) in glycerol. The high viscosity of glycerol aids to maintain the molecular orientation during the fluorescence time duration and hence enables valid anisotropy measurements. The fluoresence signal of the dyes is collected using two lenses which focus the light on a spectrometer behind a polarizer. A third half wave plate (Hwp3) is placed before

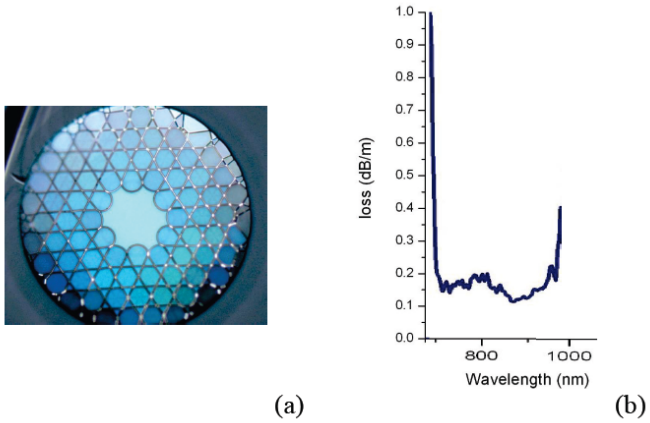

Fig. 2 Image (a) and transmission (b) of the employed kagome fiber (PMC-PL-780-USP). Data received from [13].

the fiber in order to rotate the polarization for conducting the anisotropy measurements. The anisotropy is calculated from the recorded spectra. The position of the half wave plate before the fiber is chosen in order to demonstrate the feasibility for polarization rotation after a kagome fiber since this will be realistic in endoscopic applications.

3 Results

3.1 Fiber compensation

Laser pulses were transmitted through the kagome fiber in order to determine the optical fiber properties. Thereto, the laser pulses were shaped by the pulse shaper before the fiber and detected after the fiber by using a two-photon diode. The optimization algorithm PRISM [14] was utilized to find the phase required for a transform-limited pulse at the photodiode. From the modulator settings the dispersion was determined to -406 ± 20 fs^2 for the group velocity dispersion and 7000 ± 1100 fs^3 for the third order dispersion. Hence, the fiber dispersion can well be compensated with the pulse shaper which will be conducted for all following experiments.

Fig. 3 shows the intensity behind a polarizer after the kagome fiber for different angles of the optical axes of a $\lambda/2$-waveplate positioned before the fiber for a linear input laser pulse. The slight modulation of the maxima can be attributed to polarization dependent transmission which may be due to a broken fiber symmetry since the fiber is placed in a loop on the optical table. The sinussoidal curve with intensity minima close to zero corresponds to an almost linear polarization after the fiber. Therefore, the polarization state

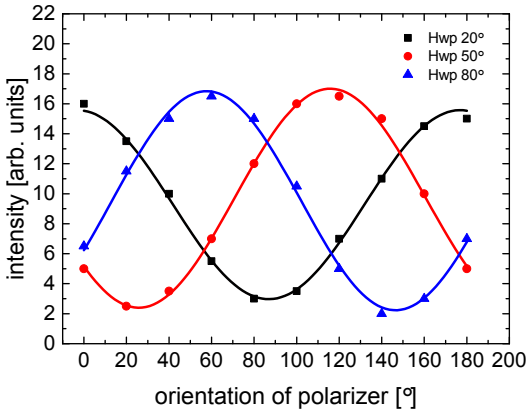

Fig. 3 Intensity behind a polarizer after the kagome fiber for different angles of the optical axes of a $\lambda/2$-waveplate (Hwp3) positioned before the fiber for a linear input laser pulse. The sinussoidal curve with intensity minima close to zero indicates an almost linear polarization after the fiber.

is nearly preserved after the fiber which allows to employ predetermined polarization shaped pulses at the distal end of the kagome fiber. In order to test the polarization stability the fiber was additionally bent in one loop with a radius of 17 cm. No significant modification was observed for the polarization state which may be explained by the large hollow core and the weak interaction only at the outer part of the laser beam profile. Hence, the polarization is relatively robust against bending which can be regarded as another advantage of the kagome fiber. However, the fiber transmission was reduced, therefore we performed the experiments without additional bending.

3.2 Pulse shapes

With the aid of the pulse shaper precompensation of the beam distortion due to the fiber is performed which enables to generate predetermined tailored laser pulses after the kagome fiber. We demonstrated this by producing laser pulses with two subpulses (according to ref. [15], alternatively the method from ref. [16] can be applied) where one subpulse is transform-limited and the other one exhibits a certain chirp. The pulse shapes were recorded by using an autocorrelator. Fig. 4 (b) shows the autocorrelation trace of a first short and a second linear chirped subpulse. A positive and a negative cubic phase for the second subpulse are depicted in fig. 4 (c) and (d), respectively. It is interesting to note that the side maxima can be regarded as cross-correlations traces of the chirped and the transform-limited subpulses. Hence, shaping of complex pulses after kagome fibers is

demonstrated since the side maxima in the cubic phase-shaped case exhibit the characteristic asymmetric features.

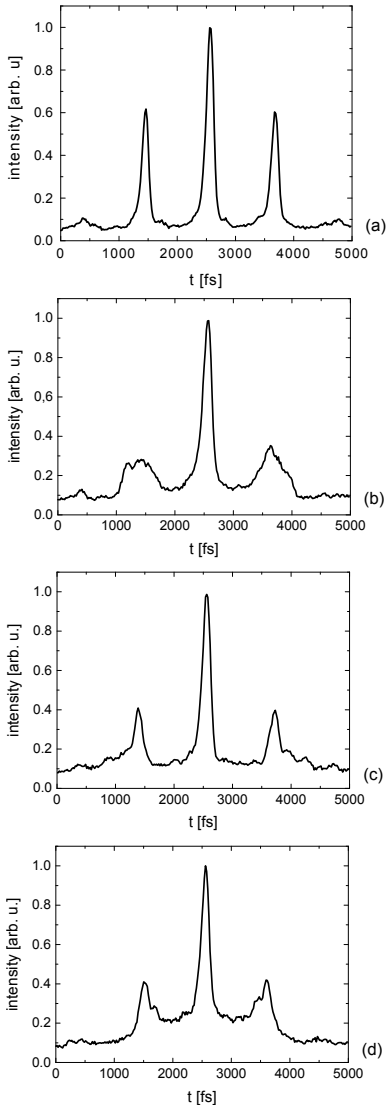

Fig. 4 Autocorrelation traces of pulse shapes with a two subpulses. (a) Double pulse with transform-limited subpulses. (b) Transfom-limited first subpulse and linear chirped second subpulse with a quadratic phase of $b_2 = 6000$ fs^2. (c) Cubic phase of $b_3 = 6{\cdot}10^5 fs^3$ for the second subpulse. (c) Cubic phase of $b_3 = -6{\cdot}10^5 fs^3$ for the second subpulse. The side maxima can be regarded as cross-correlation traces of the chirped and the transform-limited subpulses. In the cubic phase-shaped case the side maxima exhibit the characteristic asymmetric features.

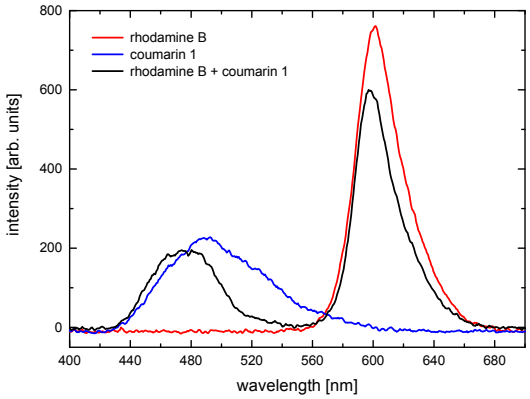

Fig. 5 Fluorescence spectra of the pure dyes rhodamine B (red line) and coumarin 1 (blue line) and the dye mixture (black line). The fluorescence for coumarin 1 in the mixture is reduced for the longer wavelengths which is interpreted by the reabsortion of light at these wavelengths by rhodamine B.

3.3 Contrast of different dyes

The pulse shaping experiments after the kagome fiber are performed on a mixture of the two dyes coumarin 1 and rhodamine B dissolved in glycerol. Particularly, two-photon excitation for both dyes was conducted with the laser central wavelength of 805 nm. The emission spectra of both dyes are well seperated which allows to distinguish between them. Fig. 5 displays the fluorescence spectra of the pure dyes compared to the dye mixture. It can be observed that the fluorescence of coumarin 1 in the mixture is reduced for the longer wavelengths compared to the pure dye which can be explained by the reabsortion of these frequencies by rhodamine B. Moreover, both dyes exhibit a high polarization anisotropy in glycerol (see Fig. 7).

Different slopes of the frequency dependent absorption yields for the two dyes enable to influence the contrast between the emissions of the dyes by phase-shaping. In order to find the pulse shapes leading to a high contrast between both dyes, cubic phase functions $\phi = \frac{b_3}{6}(\omega - \omega_0)^3$ with a third order phase scaling factor b_3 and different center frequencies ω_0 are written on the modulator. For each function the contrast k was calculated by $k = (I_{cou1} - I_{rhoB})/(I_{cou1} + I_{rhoB})$, with I_{cou1} and I_{rhoB} being the integrated intensities of the corresponding spectra. The recorded contrast for a scan of the center wavelength $\lambda_0 = 2\pi c/\omega_0$ of cubic phase functions is depicted in fig. 6. According to the contrast curve the fluorescence of coumarin 1 is higher for shorter wavelengths whereas the fluorescence of rhodamine B increases for longer wavelengths. This is due to the different slopes of the absorption curves, yet the above mentioned reabsorption in the mixture will reduce the contrast compared to pure dyes. The maximal contrast difference

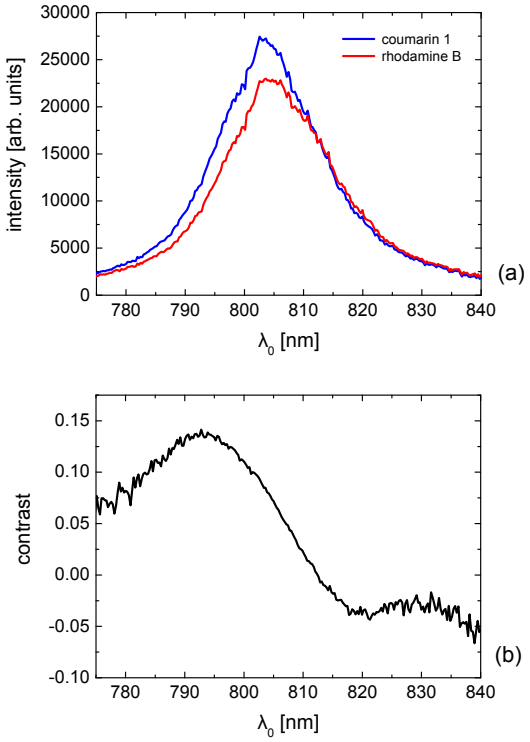

Fig. 6 Fluorescence intensities (a) and contrasts (b) for coumarin 1 and rhodamine B by scanning the center wavelength λ_0 of cubic phase functions for the scaling factor $b_3 = 4 \cdot 10^5 fs^3$.

found in these experiments is approximally 0.18, which is a measure for improved selectivity.

3.4 Polarization shaping for selective excitation after the kagome fiber

Generally, in solution the fluorophore molecules are randomly oriented. If the solution is irradiated with linearly polarized light, most of the excited molecules have transition dipole moments oriented within a range of angles close to the polarization of the light. Because the polarization direction of the fluorescence photons is in most cases again parallel to the transition dipole moment, the fluorescence will then be polarized as well, if the molecules do not lose their orientation by rotation, or other effects like fluorescent resonance energy transfer. The usual measure for the polarization of the emitted light is the anisotropy $a = (I_{\parallel} - I_{\perp})/(I_{\parallel} + 2I_{\perp})$ with the intensities $I_{\parallel}$ and $I_{\perp}$ being the two components of the fluorescence signal, which are polarized parallel and perpendicular to the exciting light. If the

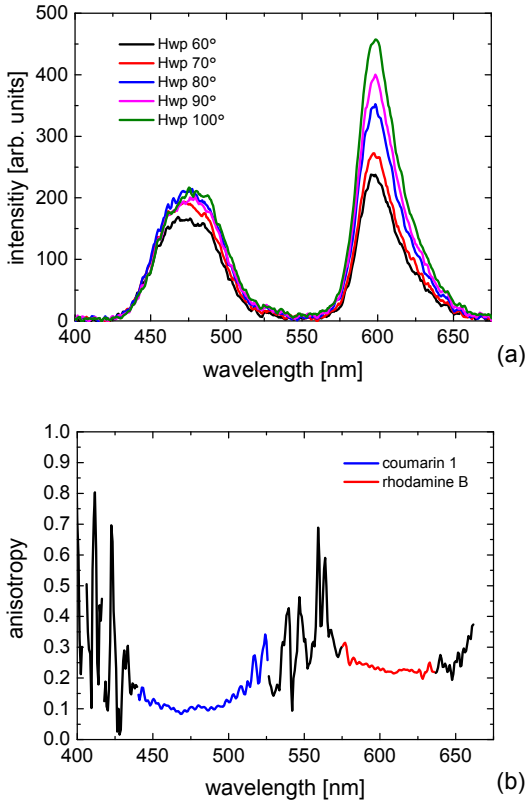

Fig. 7 (a) Emission spectra of the dye mixture for different positions of the half-wave plate measured after a polarizer. (b) Corresponding anisotropies of coumarin 1 (blue) and rhodamine B (red) are shown for different wavelengths.

fluorescence signal of fluorophores in a solution is detected behind a polarizer, the measured contrast is dependent on the orientation of the polarizer and on the anisotropy of the fluorophores.

In fig. 7 the emission spectra for different positions of the half-wave plate recorded after a polarizer and the corresponding anisotropies of coumarin 1 and rhodamine B are shown for different wavelengths. It is noticable that the anisotropy can be recorded after the kagome fiber by turning the polarization before the fiber. The anisotropy of coumarin 1 is slightly lower than the one of rhodamine B which can be explained by the faster rotation of the smaller coumarin 1 molecules and hence their diminished fluorescence yield at the initial excitation polarization state.

The emission spectra after a polarizer for the polarization shaped laser pulses are recorded at different polarization angles by tuning the half wave plate (Hwp3) orientation. The contrasts are shown in fig. 8 for an optimized laser pulse with two perpendicular polarized subpulses with a temporal

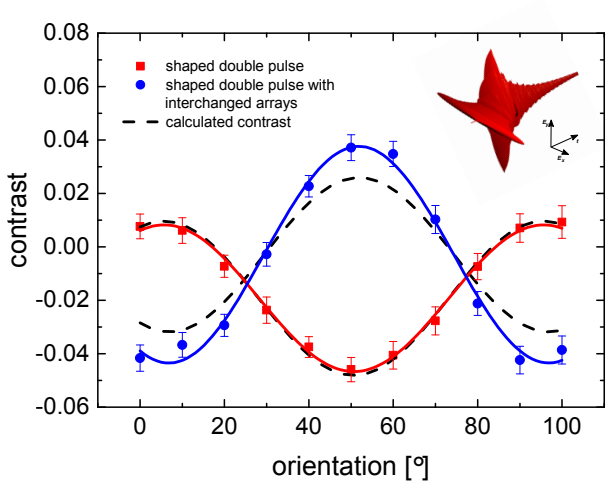

Fig. 8 Contrast between coumarin 1 and rhodamine B for the optimally phase and polarization shaped pulse (red sqares) and as well the same pulse with interchanged arrays (blue dots) depending on the rotation of the waveplate. The dashed lines display the corresponding calculations. The inset shows the calculated 3-dimensional representation of the employed phase and polarization shaped pulse.

distance of 800 fs. The slight polarization dependent transmission of the fiber was corrected by subtracting the recorded contrast of two transform-limited perpendicular subpulses. The chirp parameters for the subpulses were set such that on one array a cubic phase function $b_3 = 4 \cdot 10^5 fs^3$ with the symmetry point at 797 nm (for selective excitation of coumarin 1) and on the other array the same cubic function but with the symmetry point at 813 nm (for excitation of rhodamine B) is written on. The second experimental plot displays the results with interchanged pulse shaper arrays, which means that the subpulse with the symmetry point for selective excitation of one dye is now generated by the other array and vice versa.

Furthermore, we simulated the contrasts by calculating the two subpulse case on basis of the data for a single polarization direction from fig. 6. The contrast is maximal e.g. if the first subpulse, optimized for coumarin 1, is parallel to the polarizer. It can be written as:

$$k_{max}(I_{cou1}, I_{rhoB}) = \frac{I^1_{cou1} + \beta_{cou1} I^2_{cou1} - I^1_{rhoB} - \beta_{rhoB} I^2_{rhoB}}{I^1_{cou1} + \beta_{cou1} I^1_{cou1} + I^1_{rhoB} + \beta_{rhoB} I^2_{rhoB}}, \qquad (1)$$

where the superscripts 1 and 2 denote the subpulses by which the dyes are respectively excited, and $\beta = (1 - a)/(2 + a)$. The minimal contrast in this case is achieved by the exact opposite situation. Here the second subpulse

is e.g. parallel to the polarizer:

$$k_{min}(I_{cou1}, I_{rhoB}) = \frac{I^2_{cou1} + \beta_{cou1} I^1_{cou1} - I^2_{rhoB} - \beta_{rhoB} I^1_{rhoB}}{I^2_{cou1} + \beta_{cou1} I^1_{cou1} + I^2_{rhoB} + \beta_{rhoB} I^1_{rhoB}}. \quad (2)$$

The fluorescence intensities for the two dyes are received from the data shown in fig. 6 (a). For the different wave plate axis angles γ the contrasts are calculated by $k = 0.5(k_{max}(I_{cou1}, I_{rhoB}) - k_{min}(I_{cou1}, I_{rhoB}))cos(4(\gamma - \gamma_0))$, with γ_0 being the position of the waveplate in which the first subpulse is parallel to the polarizer. For the case with interchanged arrays the pulse numbering has to be modified accordingly.

A good agreement between simulation and experiment is obtained which demonstates the precise control over the generated pulse shape. The inset shows the calculated 3-dimensional representation of the employed phase and polarization shaped pulse. The distinct contrast difference of the polarization and phase shaped pulse demonstrates the contrast improvement by using specific phase shaped polarization components for two-photon fluorescence.

4 Conclusions

A kagome fiber was utilized for guiding polarization shaped laser pulses. It was shown that the distortion of laser pulses due to the optical fiber properties can be precompensated by using a pulse shaper. This enables to achieve predetermined tailored laser pulses after the fiber which can be employed for endoscopic applications. Moreover, the polarization of the laser pulses can be turned by rotating it before the kagome fiber which will be beneficial in endoscopic applications since no space for a half wave plate will be available after the fiber.

The anisotropy of dyes was measured and the change of the contrast between their fluorescence was demonstrated by the use of antisymmetric phase functions. In particular, we demonstrated improved fluorescence anisotropy contrast between two different dyes by two-photon excitation with polarization shaped laser pulses after a kagome fiber. It allowed us to selectively excite one dye in one polarization direction and simultaneously the other dye in the perpendicular polarization direction. This could be applied in imaging techniques and further enables e.g. to investigate the structure of tissue (collagen configuration and alignment) by polarization shaped laser pulses. The unique properties of kagome fibers with their broad transmission band, possible precompensation of their optical distortions, and the feasibility for guiding intense laser pulses are favorable for novel endoscopic applications.

5 Aknowledgement

The autors thank Prof. Wöste for support.

References

1. R. S. Judson and H. Rabitz, Phys. Rev. Lett. **68,** (1992) 1500-1503.
2. T. Brixner and G. Gerber, ChemPhysChem **4** (2003) 418-438.
3. T. Brixner and G. Gerber, Opt. Lett. **26** (2001) 557-559.
4. L. Polachek, D. Oron, and Y. Silberberg, Opt. Lett. **31** (2006) 631-633.
5. F. Weise and A. Lindinger, Appl. Phys. B **101** (2010) 79-91.
6. V. V. Lozovoy, I. Pastirk, K. A. Walowicz, and M. Dantus, J. Chem. Phys. **118** (2002) 3187-3196.
7. S. Perry, R. Burke, and E. Brown, Ann. Biomed. Eng. **40** (2012) 277.
8. F. Weise, M. Pawlowska, G. Achazi, and A. Lindinger, J. Opt. Soc. Am. B **28** (2011) 406.
9. F. Couny, F. Benabid, and P. S. Light, Opt. Lett. **31** (2006) 3574.
10. F. Emaury, C. Fourcade-Dutin, C. J. Saraceno, M. Trant, O. H. Heckl, Y. Y. Wang, C. Schriber, F. Gerome, T. Südmeyer, F. Benabid, and U. Keller, Opt. Expr. **21** (2013) 4986.
11. M. Alharbi, T. Bradley, B. Debord, C. Fourcade-Dutin, D. Ghosh, L. Vincetti, F. Gerome, and F. Benabid, Opt. Expr. **21** (2013) 28609.
12. A. Patas, G. Achazi, C. Winta, and A. Lindinger, J. Opt. Soc. Am. B **31** (2014) 2208.
13. PMC-PL-780-USP datasheet, received from GLOphotonics SAS.
14. T. Wu, J. Tang, B. Hajj, and M. Cui. Opt. Express **19** (2011) 12961.
15. S. M. Weber, A. Lindinger, F. Vetter, M. Plewicki, A. Merli, and L. Wöste, Eur. Phys. J. D **33** (2005) 39.
16. D. Pestov, V. V. Lozovoy, and M. Dantus, Opt. Express **17** (2009) 14351.